GEOMETRY BASED LOCALIZATION ALGORITHMS IN ACOUSTIC EMISSION

Václav Kůs and Petr Svojítka

Department of Mathematics, FJFI ČVUT Praha, Czech Republic

Abstract

The paper deals with the problem of localization of acoustic emission (AE) sources on general surfaces using the theory of differential geometry. More precisely, we present a localization algorithm based on the theory of geodesic curves. First, we have a look at the theoretical background of the problem, which is particularly the geodesic equations and the method of obtaining their solution. Next, the localization algorithm itself is described. At the end of the paper, the implementation of the algorithm to the model of a pressure vessel with incoming pipelines is shown and test results are presented.

Keywords: Acoustic emission, localization, geodesic curves, statistics, experiment

INTRODUCTION AND THEORETICAL MODEL

AE source localization is based on the knowledge of time differences which are detected by AE sensors. We presume, that the positions of three AE sensors are known and so are the respective time differences. With the known speed of elastic wave propagation in a given material, these time differences are expressed as length differences, which is more convenient for the localization algorithm.

We assume, that the surface of the object, which is to be tested, can be modelled as a composition of a certain number of given parametrized surfaces. This is a legitimate presumption. Typical objects, which are tested by AE techniques, are various cylindrical pressure vessels, spherical reservoirs, incoming pipelines etc.

We reduce all the theory of geodesic curves and differential geometry just on stating those basic facts, that are necessary for finding geodesic curves and thus for finding the shortest connection of two points laying on some given surface (see [1] or [2] for more details).

We work with parametrized surfaces given by means of a differentiable mapping $\mathbf{x} : U \to M \subset \mathbb{R}^3$ such that

$$\mathbf{x}(u,v) = (x_1(u,v), x_2(u,v), x_3(u,v)),$$

where $(u,v) \in U \subset \mathbb{R}^2$. Similarly, a parametrically given curve in $\mathbb{R}^3$ is a differentiable mapping

$$\alpha : (a,b) \to \mathbb{R}^3, \qquad \alpha(t) = (a_1(t), a_2(t), a_3(t)),$$

where (a,b) is an interval in $\mathbb{R}$. It's clear, that a curve α lies on the surface M, if $\alpha(t) \in M$ for $\forall t \in (a,b)$.

A curve α laying on a surface M is called geodesic, if the tangent element of the vector α'' vanishes (the mapping α is differentiated in an ordinary way, element by element). Geodesic curves can be defined also in other ways, for example as a locally shortest path connecting two points. Geodesic actually is a generalization of the notion of a straight line to curved spaces. The crucial property for us is, that the shortest path connecting two points of a surface is a geodesic curve (but the reverse implication generally doesn't hold). Thus, if we find the length of the shortest geodesic curve connecting two given points onto a surface, we find the distance of these points measured along the surface.

We are trying to find geodesic curves in the form

$$\alpha(t) = \mathbf{x}(u(t), v(t)).$$

The mathematical theory concerning differential geometry provides us with a set of two geodesic equations, which the geodetic curves have to satisfy. The equations have a compact form

$$\begin{aligned} u'' + \Gamma^1_{11}u'^2 + 2\Gamma^1_{12}u'v' + \Gamma^1_{22}v'^2 &= 0, \\ v'' + \Gamma^2_{11}u'^2 + 2\Gamma^2_{12}u'v' + \Gamma^2_{22}v'^2 &= 0, \end{aligned}$$

where Γ^i_{jk} are so called Christoffel symbols, which carry the information about the given surface. Before they can be defined, three functions have to be introduced $E, F, G : U \to \mathbb{R}$ as

$$E = \|\mathbf{x}_u\|^2, \quad F = \mathbf{x}_u \cdot \mathbf{x}_v, \quad G = \|\mathbf{x}_v\|^2,$$

where $\mathbf{x}_u, \mathbf{x}_v$ are partial derivatives of $\mathbf{x}$ with respect to u and v. With use of these functions, the Chrisoffel symbols are given by

$$\begin{aligned} \Gamma^1_{11} &= \frac{GE_u - 2FF_u + FE_v}{2(EG - F^2)}, & \Gamma^2_{11} &= \frac{2EF_u - EE_v - FE_u}{2(EG - F^2)}, \\ \Gamma^1_{12} &= \frac{GE_v - FG_u}{2(EG - F^2)}, & \Gamma^2_{12} &= \frac{EG_u - FE_u}{2(EG - F^2)}, \\ \Gamma^1_{22} &= \frac{2GF_v - GG_u - FG_v}{2(EG - F^2)}, & \Gamma^2_{22} &= \frac{EG_v - 2FF_v + FG_u}{2(EG - F^2)} \end{aligned}$$

and $\Gamma^1_{21} = \Gamma^1_{12}$, $\Gamma^2_{21} = \Gamma^2_{12}$.

NUMERICAL COMPUTATIONS AND TESTS

Geodesic equations forms a set of two nonlinear ordinary differential equations with boundary conditions. The equations are solved by a relaxation iterative method, where the derivatives are substituted with finite difference quotients. An equation of the form $y'' = f(x, y, y')$ is substituted by the difference equations

$$y_{i+1} - 2y_i + y_{i-1} = (\triangle x)^2 f(x_i, y_i, \frac{y_{i+1} - y_{i-1}}{2(\triangle x)}),\ i = 2, \ldots, M-1,$$

where $y(x_i) = y_i$. Coupled with two boundary conditions, we get a set of equations with a tri-diagonal matrix for y_i. This set is solved by gaussian elimination. For more details see [3].

As the tested object is modelled by a composition of given parametrized surfaces, we are trying to find geodesic curve connecting two points laying on different parametrical surfaces. So the resulting geodesic curve have to cross the intersection of those surfaces on its way from the starting point to the end point. The length of this resulting curve is the distance of those points measured along the surfaces (an example can be seen on Figure 1).

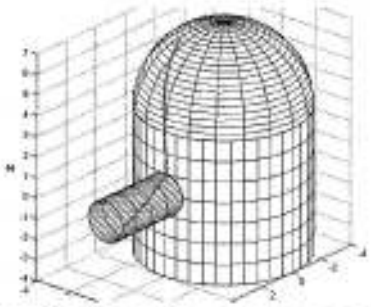

Figure 1: An example of a geodesic curve on a compound surface

Numerical approach is as follows. An uncountable set of intersection of two surfaces (boundary-line between the two surfaces) is transformed into a discrete set of divisive points. For every splitting point the length to the starting point along the first surface is computed as well as the length to the end point along the second surface. These lengths are summed up together, which gives the length of the shortest curve crossing this exact point of the intersection. And since this is done for every divisive point of the set, the searched shortest distance can be selected. The more divisive points we are working with, the more precise the result is. On the other hand, the increasing amount of the tested points on the surface boundary-line increases also the time necessary for finding the geodesic curve. So the number of the divisive points has to be chosen deliberately.

Now we describe the basic idea of the localization. First, the area which is to be tested has to be determined, i.e. intervals for parameters describing a tested surface are chosen (that means that the determination of the tested area is dependent on the specific topology of a tested object). Both intervals are then split into a certain number of points, which

covers the tested area with a rectangular computational grid. The grid division need not be equidistant in general. Next, every cross-point of the grid is tested. Distances to the sensors are counted from each knot, which gives us the lengthwise differences corresponding to that grid-point. These differences are confronted with the input lengthwise differences and based on the level of coincidence it is determined, if the actual point of the grid is a potential AE source or not.

The length differences respective to the actual grid-point i are confronted with the input length differences (let's denote them $\triangle s_{12}$, $\triangle s_{13}$, $\triangle s_{23}$), respective to the time differences, which were detected by the sensors. Let I be a set of all cross-points of the grid, for every $i \in I$ we denote the obtained differences as

$$\triangle s^i_{12} = s^i_2 - s^i_1, \quad \triangle s^i_{13} = s^i_3 - s^i_1, \quad \triangle s^i_{23} = s^i_3 - s^i_2,$$

where s^i_1, s^i_2 and s^i_3 are distances of the vertex i from the sensors 1, 2 and 3. We select to be a potential AE source such a vertex $i \in I$, for which is the standard distance

$$d_i = \sqrt{(\triangle s_{12} - \triangle s^i_{12})^2 + (\triangle s_{13} - \triangle s^i_{13})^2 + (\triangle s_{23} - \triangle s^i_{23})^2}$$

minimal. Time differences are dependent on each other, i.e. the two of them determine the third one uniquely. For this reason, it should be enough to work just with two differences, for example the third term $(\triangle s_{23} - \triangle s^i_{23})^2$ could be omitted from the definition of the norm. But as it is shown in one of the following tests, the localization with such norm has different properties.

LOCALIZATION no. 1

Now we apply the above described algorithm and methods to the model of specific vessel - the pressure boiler of cylindric shape with the diameter 4 meters and with several incoming pipes, which have also cylindric and they are connected directly and rectangularly to the boiler vessel (i.e. the incoming pipe axis is rectangular to the axis of boiler). All the incoming pipes have the same diameter $0,6$ m and the AE sensors on the top of acoustic waveguide are placed on them.

Three pipes with sensors were selected and input data sets were generated in order to localize the AE source. First, we choose the point on the vessel surface representing the source of emission signals and consequently we count its distance from every single considered sensors. We produce the input data form precise differences by adding additive noise in the form of random variable X with the normal (Gauss) distribution with zero expectation EX. We prepared 20 different input data sets by this procedure. We applied our localization algorithm to every data set and thus we obtained 20 corresponding AE source localization points on our surface of vessel considered in this experiment. Then, the resulting statistical localization of the AE source was determined as the center of gravity of these 20 founded separated localization points. This approach corresponds to some real measurement situation where the statistical localization based on reasonable high number of noisy real signals is quite

necessary (the only one localization from the single data set of differences is nonsensical in this case).

In this testing, the AE source which should have been detected by the algorithm, was positioned in the middle between the three selected incoming pipes with sensors. The shortest trace from this point to the sensors can be seen in Figure 2.

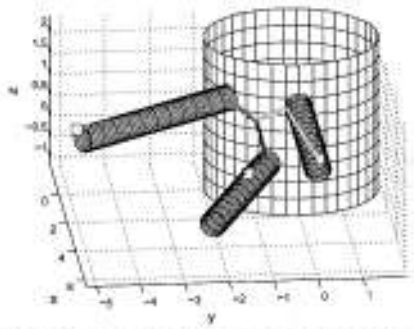

Fig. 2: Localization test no. 1 and AE source position

The considered area of the testing vessel was covered by the computational rectangular grid with the gap between the neighbouring knots 4 cm in vertical direction and approximately 3,9 cm in horizontal direction. Notice that our AE source do not coincide with any grid points.

First, we tested the algorithm for all 20 data sets using only two differences, i.e. the following norm have been used $\sqrt{(\triangle s_{12} - \triangle s'_{12})^2 + (\triangle s_{13} - \triangle s'_{13})^2}$.

The single localization points can be seen in Figure 3. The square mark denotes the real position of AE signal source, the circles denote the obtained localizations and the cross gives the position of the resulting statistical localization. If the circle is doubled in diameter this means that the same grid point include two localizations. The figured subarea of surface of the vessel has approximately the real size 35×35 cm. The distance of our statistically localized source (cross) from the real AE source (square) is $1,7$ cm (measured onto the cylindric surface).

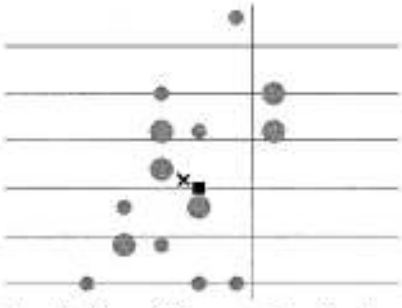

Fig. 3: Two differences localization

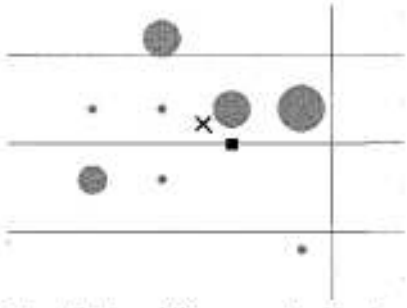

Fig. 4: Three differences localization

The same 20 input data sets were consequently used again for similar experiment but with the norm including all the three differences

$$\sqrt{(\triangle s_{12} - \triangle s_{12}^i)^2 + (\triangle s_{13} - \triangle s_{13}^i)^2 + (\triangle s_{23} - \triangle s_{23}^i)^2}.$$

The points obtained are presented in Figure 4. This time, two or more localizations belong to the same grid-knot, that is why the diameters of circles are now proportional to the number of localizations in grid points in Figure 4. The figured subarea of surface of the vessel has approximately the real size 20×20 cm in this case.

The first sight onto Figure 4 reveals that the localizations corresponding to separated input data sets are more concentrated around real source than in the previous case. The distance of our statistically localized source (cross) from the real AE source (square) is now $2,24$ cm (measured onto the cylindric surface) and it is sufficiently accurate. In spite of the fact that this localization is a little worse then that of Figure 3, we can see that the statistical variance of these localization points is reduced down, which is considered to be essential.

In this described mathematical experiment the localization setup was favourable (the closest incoming pipes with the source in the middle of them). In the following section we explore the setup which is not so appropriate.

LOCALIZATION no. 2

In this case we seek for the AE source by means of the sensors placed on the pipes which were rather remoted from each other. Moreover, the AE source was selected relatively close to the couple of pipes and relatively far from the third incoming pipe (see Figure 5).

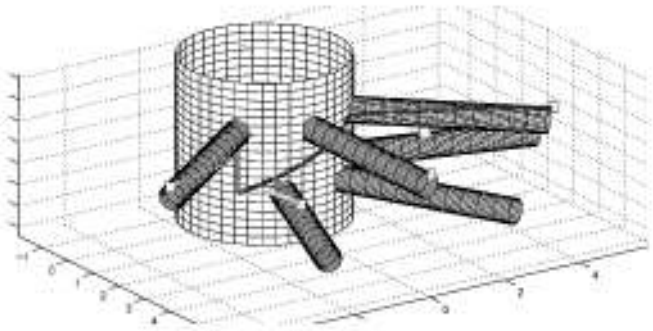

Fig. 5: Localization test no. 2 and AE source position

Also in this case, 20 different input data sets were produced and the normal noise was additively added to them. Now, we do not sum the noisy random variable to the time differences but we add the noise directly to the distances of the chosen source from the single sensors. Moreover, the variances of this normal random noises were different for every considered distance. This approach corresponds well with the real situations where the greater error term can be expected for more distant service incoming pipes. The results of this

localization are presented in Figure 6 where the real height of figured region is approximately 3,5 m.

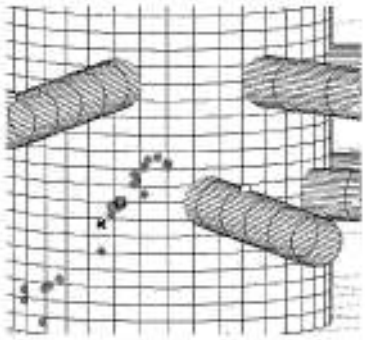

Obr. 6: Results of statistical localization no. 2 on the vessel

The distance of statistically localized AE source from the real source of AE signals is here 33,3 cm. From this value and from the Figure 6 it can be seen clearly that the localization is considerably inaccurate in this case particularly in comparison with the first localization setup. However, we could expect such results for this second test, because the localization procedure is now very sensitive to the error terms in input data sets for such positions of incoming pipes when the only one of them is far from the others and the AE source is between the two closest remaining pipes. Thus even a small change in distance differences results in great shift of the localized points and thus we conclude that the statistical feature of the mean value localization is quite necessary.

COMPUTATIONAL TIMES

Computational time of the presented localization depends mainly on the number of points of the computational grid. Further factor which has an influence is the number of points to which we split the boundary-line intersection between the particular surfaces. To illustrate this fact we select the area 2×2 m on the solid body shell and we explore the influence of the computational time for this region on the mentioned factors. We tabulate approximate computational times changing the grid step and the number of divisive points onto the boundary-line in Table below. The tabulated test-times were computed for the case of PC Pentium M 1.7MHz.

			grid step	
		10 cm	5 cm	2,5 cm
	10 cm	38 s	145 s	580 s
boundary step	5 cm	75 s	290 s	1200 s
	2,5 cm	150 s	600 s	24000 s

CONCLUSION

The presented localization method of AE sources can be very precise because we can choose both, the step of computation grid and the number of splitting points on boundary-line between surfaces, quite arbitrary. But this precision goes against the computational time and therefore we are forced to seek for some new ways of accelerating the presented algorithm.

This project is supported by the grant MPO FI-IM3/136.

References

[1] Alfred Gray. *Modern Differential Geometry of Curves and Surfaces.* CRC Press, Boca Raton, Florida, 1993.

[2] Manfredo P. do Carmo. *Differential Geometry of Curves and Surfaces.* Prentice-Hall, New Jersey, 1976.

[3] Emil Vitásek. *Numerické metody.* SNTL, Praha, 1987.

[4] Petr Svojítka, Václav Kůs. *Geodetické lokalizační algoritmy pro obecné povrchy těles.* Technická zpráva na Katedře matematiky FJFI, Praha, 2007.